Int. J. Electrochem. Sci., 12 **(2017)** 3589 – 3596, doi: 10.20964/2017.05.77

International Journal of
ELECTROCHEMICAL
SCIENCE
www.electrochemsci.org

Short Communication

One-Step Hydrothermal Synthesis of Nickel/Cobalt Double Hydroxide Composite Containing Reduced Graphene Oxide as High Perfomance Electrode Material for Supercapacitor

Guoping Wang[1,*], *Hui Jia*[1], *Liwei Zhu*[1], *Meirong Li*[2], *Yurong Ren*[2,*], *Yanjie Wang*[3]

[1] College of Chemistry and Chemical Engineering, University of South China, Hengyang, Hunan 421001, China
[2] School of Materials Science and Engineering, Jiangsu Collaborative Innovation Center for Photovoltaic Science and Engineering, Changzhou University, Changzhou 213164, China.
[3] Department of Chemical and Biological Engineering, University of British Columbia, 2360 East Mall, Vancouver, BC Canada V6T1Z3
[*]E-mail: ryrchem@163.com, wgpcd@aliyun.com, wgpcd@yahoo.com.cn

Received: 5 December 2016 / *Accepted:* 28 February 2017 / *Published:* 12 April 2017

Nickel/cobalt double hydroxide composite containing reduced graphene oxide (Ni/Co-DH-RGO) with high electrochemical performances has been prepared by hydrothermal one-step method accompanied with using hexamethylene tetramine (HMT) as homogeneous precipitating agent and its hydrolysis product for reducing graphene oxide. X-ray diffraction pattern displays that Ni/Co-DH-RGO exists as a composite of α-$Ni(OH)_2$-β-$Co(OH)_2$ and reduced graphene oxide. Infrared spectrum shows that the typical peaks of carboxyl and expoxy group in graphene oxide are significantly weakened after the hydrothermal reaction. Scanning electron microscope image shows Ni/Co-DH-RGO takes on hierarchical morphology. The as-prepared Ni/Co-DH-RGO has a specific capacitance of 2120 F g^{-1} at a current density of 1A g^{-1} and 1569.8 F g^{-1} at the current density of 8 A g^{-1}.

Keywords: Hydrothermal one-step synthesis; Hexamethylene tetramine; Nickel/cobalt double hydroxide composite; supercapacitor; electrode material.

1. INTRODUCTION

Metal hydroxides, as promising supercapacitor electrode materials, have attracted increasing attention because of their large specific capacitance, high energy density, and environmental friendliness [1,2]. However, they suffer from low electron and ion conductivity, which restricts their practical applications in high-performance supercapacitors.

To address the above issue, some efforts have been attempted. For example, carbon materials, such as active carbon [3], carbon nanotubes [4], graphene [5], and carbide-derived carbon [6] etc., are used as electrical conductivity additives in metallic hydroxide electrode. Especially, graphene has attracted more and more attention, owing to its higher ballistic conductivity and bigger specific surface area [7].

Generally, to achieve high electron conductivity, graphene oxide (GO) is firstly reduced in a separate device before forming a composite with metallic hydroxide [8-14]. However, the separate reduction processes can decrease carboxylic acid, epoxy and hydroxyl groups in GO, resulting in unavoidable aggregation of GO and in turn the difficulty in loading metallic hydroxide. Meanwhile, such separate reduction process is always time-consuming and not economical. Therefore, new methods or new reductants are necessary for synthesizing reduced graphene oxide (RGO)/metallic hydroxide composites. Besides, metallic hydroxides like nickel/cobalt double hydroxide (Ni/Co-DH), are often synthesized by adding the precipitant ammonia water drop by drop in references. Obviously, such a process is very difficult to operate and not convenient.

Therefore, it is necessary to prepare metallic hydroxide composite in an economical way and a simple process. In this paper, hydrothermal reactor was used in combination with utilizing homogeneous precipitating agent.

Hydrothermal method is time-saving and very simple to operate in addition to being able to conveniently control the morphology and size of materials [15,16]. It is widely adopted to prepare materials with desirous properties. Using the homogeneous precipitating agent can produce the precipitating agent slowly in the reactive process, avoiding the cumbersome process of adding alkali.

Hexamethylene tetramine (HMT) can be hydrolyzed into ammonia and formaldehyde in hydrothermal reactor (autoclave), which can act as a homogeneous precipitating agent and a reductant, respectively. When the reductant formaldehyde reduces GO, metal hydroxides can deposit simultaneously on the surface of GO. The synergistic effect induced by composites may prevent GO particles' agglomeration. As a result, not only can GO be easily reduced in the hydrothermal process and the aggregation of GO be alleviated, but also it is not necessary to add alkali drop by drop for preparing metallic hydroxide.

In this work, we have tried to prepare Ni/Co-DH-RGO by hydrothermal one-step process accompanied with using HMT as homogeneous precipitating agent. Neither additional reductant nor additional alkali is needed. The preparing process of Ni/Co-DH-RGO composite is greatly simplified, and the as-prepared Ni/Co-DH-RGO shows excellent electrochemical performance.

2. EXPERIMENTAL

2.1. Synthesis of the composite

Firstly, 20 mg GO was dispersed ultrasonically in 50 ml deionized water for 1 h to form homogeneous GO solution. Then, 0.2908 g of $Ni(NO_3)_2 \cdot 6H_2O$ and 0.2911 g of $Co(NO_3)_2 \cdot 6H_2O$ were dissolved in the GO solution. This solution was transferred into a 100 mL autoclave. Hereafter, 1 g HMT was added, and the autoclave was maintained at 105 °C for 2 h. After being naturally cooled down to room temperature, Ni/Co-DH-RGO was washed with deionized water and alcohol for several

times, and then dried at 60 ℃ in a vacuum oven for 8 h. For comparison, nickel and cobalt double hydroxide (Ni/Co-DH) and RGO were also prepared separately with the above process.

2.2. Structure characterization and electrochemical evaluation

The scanning electron microscope (SEM) image was obtained using a Hitachi S4800 SEM (Hitachi, Japan). X-ray diffraction (XRD) pattern was measured on X-ray D/max-2200 vpc instrument operated at 40 kV and 20 mA using Cu Kα radiation source with λ = 0.15406 nm. Infrared spectra (IR) were recorded on a FT-IR (Shimadzu, Japan). Cyclic voltammetry (CV), galvanostatic charge-discharge (GCD) and electrochemical impedance spectrums (EIS) were performed on a CHI660E electrochemical workstation (Huakeputian Beijing, China) with a three-electrode system, where Pt electrode and Hg/HgO electrode were served as the counter electrode and reference electrode, respectively. The working electrode was prepared as the reference [17] (geometric surface area is 0.07 cm^2). All electrochemical measurements were carried out at room temperature (23±2 °C) in 6.0M KOH electrolyte solution.

3. RESULTS AND DISCUSSION

3.1. Material characterization

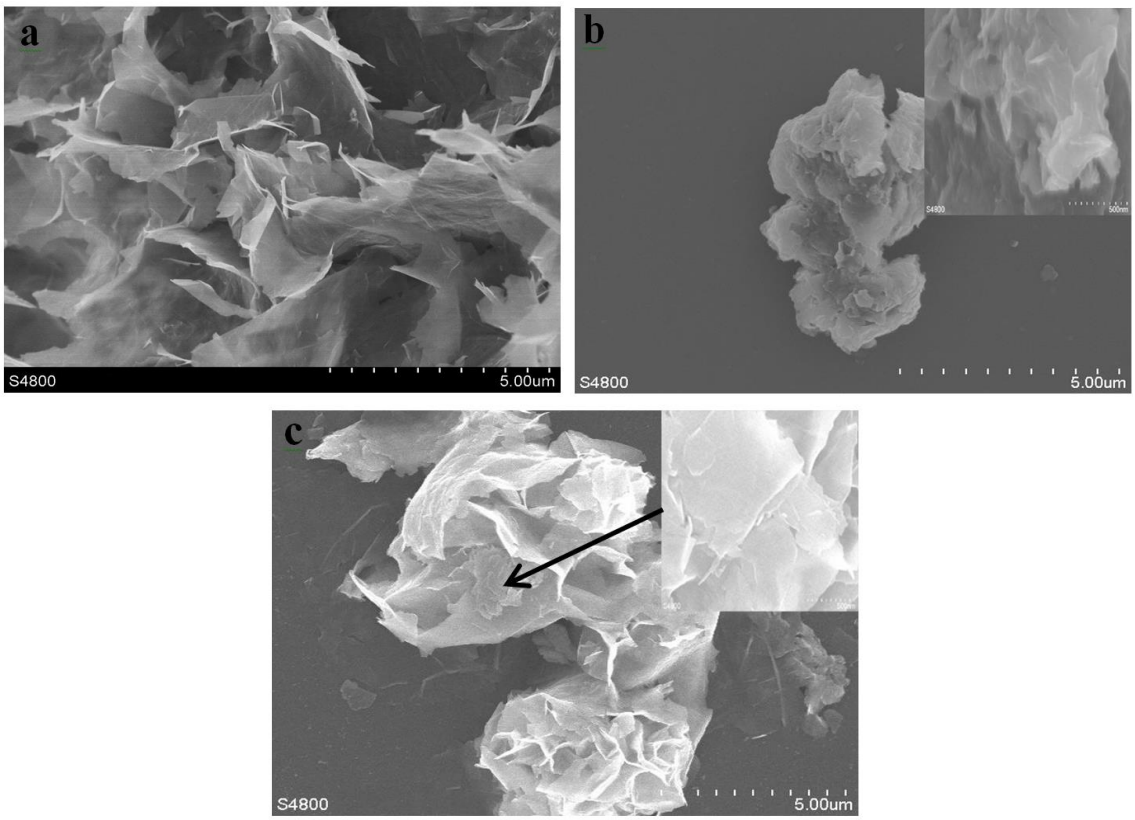

Figure 1. SEM images of (a) RGO, (b) Ni/Co-DH and (c) Ni/Co-DH-RGO.

As shown in Fig. 1, the obtained RGO looks like leaves. Ni/Co-DH shows layered structure. If forming composite with RGO, Ni/Co-DH randomly deposits on the RGO surface, but the pores in the composite Ni/Co-DH-RGO remain as well as in RGO. As report in previous work [18], Ni/Co-DH and RGO sheets are interlinked with each other, forming layer on layer structure, the structure and pores provide excellent electron-diffusion paths, thus facilitating the diffusion and migration of electrolyte ions within electrode materials and enhancing the electrochemical behavior of the composite.

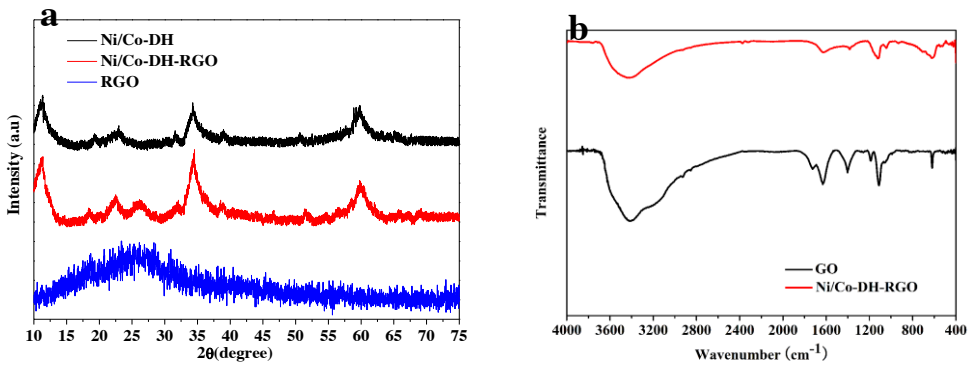

Figure 2. (a) XRD patterns of RGO, Ni/Co-DH and Ni/Co-DH-RGO (b) IR patterns of GO and Ni/Co-DH-RGO.

The XRD patterns of the as-prepared Ni/Co-DH-RGO, Ni/Co-DH and RGO are depicated in Fig.2(a). Ni/Co-DH-RGO and Ni/Co-DH display some similar XRD patterns to certain extent. Both of them present four main characteristic peaks, which suggest that Ni presents in the form of α-$Ni(OH)_2$ and Co in β-$Co(OH)_2$ [19]. The peaks at 11.3°, 22.7°, 34.5° and 60.0° are indexed to the rhombohedral phase of $Ni(OH)_20.75H_2O$ (JCPDS:38-0715), which correspond to the (003), (100), (101) and (110) planes, respectively. The peaks at 19.2°, 32.5°, 38.7° and 51.4° are indexed to the hexagonal phase of $Co(OH)_2$ (JCPDS:30-0443), which correspond to the (001), (100), (101) and (102) planes, respectively. Comparing the XRD patterns of Ni/Co-DH-RGO and RGO, a typical RGO peak at 25.6° can be observed in XRD patterns of Ni/Co-DH-RGO. Therefore, the Ni/Co-DH-RGO sample can be identified as a composite of α-$Ni(OH)_2$-β-$Co(OH)_2$ and reduced graphene oxide.

Fig. 2(b) shows IR spectra of GO and Ni/Co-DH-RGO. For GO, it presents two obvious peaks at around 1720 and 1190 cm^{-1}, which are assigned to the absorption of stretching vibration of $\upsilon_{(C=O)}$ in carboxyl and $\upsilon_{(C-O)}$ in expoxy group, respectively. Meanwhile, it displays obvious peaks at 3395, 1402 and 1111 cm^{-1}, which are the absorption of $\upsilon_{(O-H)}$ stretching and deformation vibration and $\upsilon_{(C-O)}$ stretching vibration in alkoxy, respectively. However, for Ni/Co-DH-RGO, the above peaks appeared in GO are significantly weakened or almost disappear, indicating that the oxygen-containing functional groups on GO are reduced to some extent in the process of hydrothermal reaction in the presence of HMT.

3.2. Electrochemical properties

Fig. 3(a) shows the CV curves of the Ni/Co-DH-RGO and Ni/Co-DH in 6 M KOH electrolyte at the scan rate of 5 mV s^{-1}. Obviously, Ni/Co-DH-RGO electrode shows higher current and larger

integration area than Ni/Co-DH electrode. This suggests that Ni/Co-DH-RGO electrode possesses higher specific capacitance when compared with Ni/Co-DH electrode. Besides, Ni/Co-DH-RGO electrode displays smaller potential peak separation between the anodic and cathodic peak than Ni/Co-DH electrode, indicating its lower polarization. As reported in previous work [20], the small peak-to-peak separation value may be due to the unique architecture of the Ni/Co-DH-RGO greatly improves the Faradaic redox reaction. Similar results can be observed from the charge/discharge curves. As shown in Fig. 3(b), owing to the more complete redox reactions in Ni/Co-DH-RGO electrode, the charge/discharge plateau and the total charge/discharge time of Ni/Co-DH-RGO electrode are much longer than those of Ni/Co-DH electrode. Moreover, Ni/Co-DH-RGO electrode shows a gentler charge/discharge curve than Ni/Co-DH electrode, further testifying the lower polarization of Ni/Co-DH-RGO electrode. Such phenomena may be attributed to the higher electron conductivity of Ni/Co-DH-RGO electrode, which has been affirmed by the impedance plots. Compared with the previous literature [21,22], the as-prepared Ni/Co-DH-RGO has a larger specific capacitance.

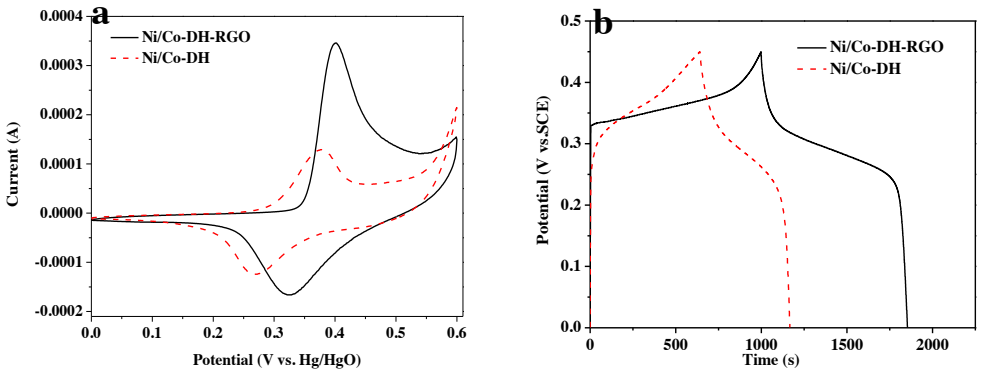

Figure 3. (a) CV curves of Ni/Co-DH-RGO and Ni/Co-DH at scan rate of 5 mV s^{-1}. (b) Charge/discharge curves of Ni/Co-DH-RGO and Ni/Co-DH at a current density of 1A g^{-1}.

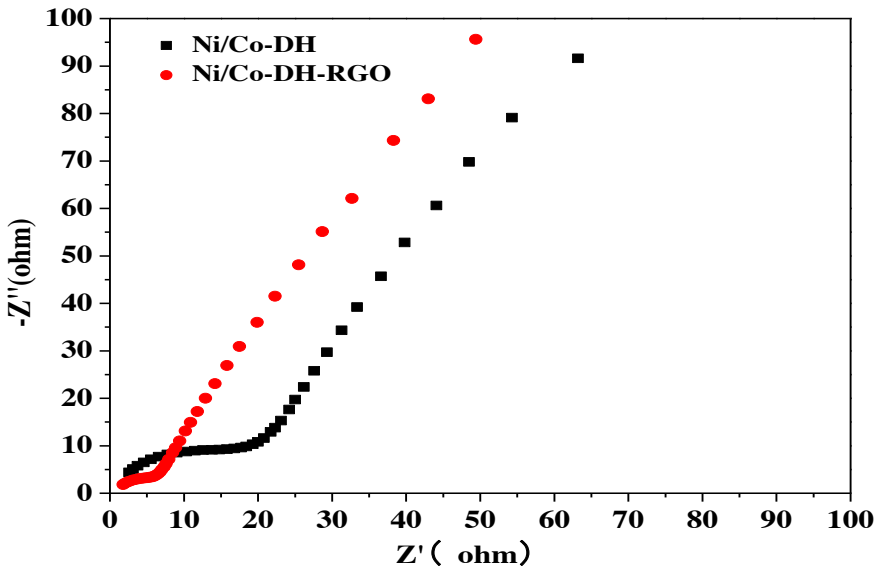

Figure 4. Impedance plots of Ni/Co-DH-RGO and Ni/Co-DH.

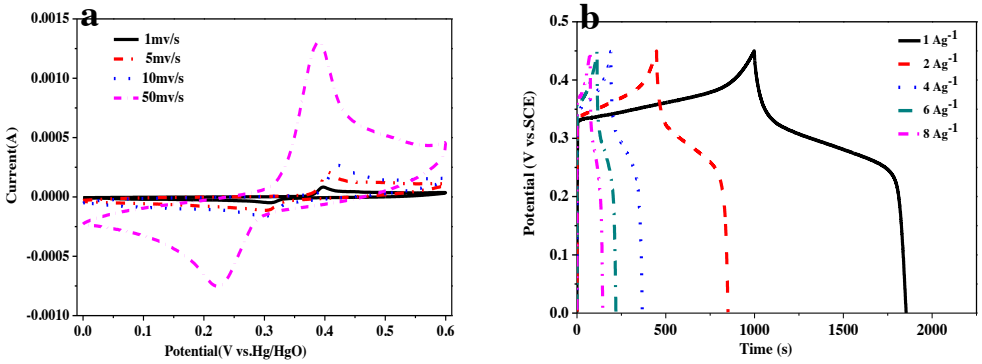

Figure 5. (a) CV curves of Ni/Co-DH-RGO at different scan rates in 6 M KOH electrolyte. (b) Charge/discharge curves of Ni/Co-DH-RGO at different current density.

Generally, the straight line in the impedance plots is associated with the diffusion rate of the electroactive species into the porous network structure of electrode. In Fig. 4, both curves present a straight line at low frequency, and the two straight lines are almost parallel. This means that Ni/Co-DH-RGO and Ni/Co-DH have similar pore structure and then comparative diffusion resistance. However, when it comes to high frequency, the semicircles of the two curves are completely different. The semicircle reflects the charge-transfer resistance at the interface. The larger the semicircle is, the larger charge-transfer resistance. Obviously, Ni/Co-DH-RGO electrode shows much smaller semicircle than that of Ni/Co-DH electrode, implying its lower charge-transfer resistance. According to the impedance plots, the calculated charge-transfer resistances of Ni/Co-DH-RGO and Ni/Co-DH electrodes are 4.21 and 14.01Ω, respectively.

Fig. 5(a) shows the CV curves of the Ni/Co-DH-RGO in 6 M KOH electrolyte at various potential scan rates. The Ni/Co-DH-RGO electrode displays a strong complementary redox peaks. Although the width of both anodic and cathodic peaks broadens with increasing potential scan rate, the widths are very close. According to CV, the specific capacitance based on the weight of Ni/Co-DH can be calculated as 2049 , 1820 , 1484 , 657 F g^{-1} at 1, 5, 10, 50 m Vs^{-1}, respectively. The decreasing trend of specific capacitance may be attributed to the limited ion transfer rate. As described in the literature [23], the ion transfer rate becomes very slowly at high scan rate. Therefore, only the external active surface of the electrode material can be utilized for charge storage during the redox process, which results in the decrease of specific capacitance. Similarly, from the charge/ discharge curves (Fig. 5(b)), the specific capacitance of Ni/Co-DH-RGO was 2120, 1962, 1804, 1749, 1570 F g^{-1} at 1, 2, 4 , 6 , 8 A g^{-1}, respectively. The specific capacitances gradually decrease with the increase of the discharge current density, which can be attributed to the electrochemical polarization. Other works mentioned that electrolyte diffusion and reaction need reduced time, thus the outer surface can be utilized for charge storage at high current density [24,25].

4. SUMMARY AND CONCLUSIONS

In this work, Ni/Co-DH-RGO has been synthesized by hydrothermal one-step synthesis method in combination with using homogeneous precipitating agent. The Ni/Co-DH-RGO based electrode can

have a specific capacitance of 2120 F g^{-1} at 1 Ag^{-1}. Combining hydrothermal one-step synthesis with homogeneous precipitating method may be an efficient way to prepare Ni/Co-DH-RGO hybrid material with excellent electrochemical performance.

ACKNOWLEDGEMENTS
The authors would like to thank the financial support Project of 2014GK3091 from Hunan Provincial Science & Technology Department.

References

1. G. P. Wang, L. Zhang , J. J. Zhang , *Chem. Soc. Rev.* ,41 (2012) 797.
2. X. Y. Yan , X. L. Tong , J. Wang , C.W. Gong, M. G. Zhang, L. P. Liang , *J. Alloys Comp.* ,593 (2014) 184.
3. M. Sevilla, R. Mokaya , *Energy & Environmental Science.* , 7 (2014) 1250.
4. G.Z. Sun, L.X. Zheng, Z.Y. Zhan, J. Y. Zhou, X.B. Liu, L. Li, *Carbon.* , 68 (2014) 748.
5. T. Kim, G. Jung, S. Yoo, K. S. Suh , R. S. Ruoff, *ACS Nano.* , 7 (2013) 6899.
6. Z. Li, L. Zhang, B. S. Amirkhiz, X. H. Tan, Z. W. Xu, H. L. Wang, B. C. Olsen, C. M. B. Holt, D. Mitlin, *Advanced Energy Materials.* , 2 (2012) 431.
7. M. Pumera, Chem. Soc. *Rev.,* 39 (2010) 4146.
8. S. J. Park, Y. C. Hu, J. O. Hwang, E. S. Lee, L. B. Casabianca, W. W. Cai, J. R. Potts, H. W. Ha, S. S. Chen, J. H. Oh, S. O. Kim, Y. H. Kim, Y. Ishii, R. Ruoff, *Nature Communications.,* 3 (2012) 638.
9. M. Yu , J. P. Chen, Y. X. Ma, J. D. Zhang , J. H. Liu, S. M. Li, J. W. An, Appl. Surf. *Sci.,* 314 (2014) 1000.
10. M. Sawangphruk, P. Srimuk, P. C. A. Krittayavathananon, S. Luanwuthi, J. Limtrakul, *Carbon.,* 60 (2013) 109.
11. W. L. Yang, Z. Gao, J. Wang, B. Wang, Q. Liu, Z. S. Li, T. Mann, P. P. Yang, M. L. Zhang, L. H. Liu, *Electrochim. Acta.* , 69 (2012) 112.
12. A. Nekahi, P. H. Marashi, D. Haghshenas, *Appl. Surf. Sci.* , 295 (2014) 59.
13. J. Tang, T. Wang, X. Sun, Y. Y. Hu, Q. Q. Xie, Y. X. Guo, H. R. Xue, J. P. He, *Electrochim. Acta.* , 90 (2013) 53.
14. L. B. Ma, X. P. Shen, Z. Y. Ji, G. X. Zhu, H. Zhou, *Chem. Eng. J.* , 252 (2014) 95.
15. M. Talebi-Esfandarani, O. Savadogo, *Solid. State. Ionics.* , 261 (2014) 81.
16. A. Sierra-Fernandez, L. S. Gomez-Villalba, O. Milosevic, R. Fort, M. E. Rabanal, *Ceram. Int.* , 40 (2014) 12285.
17. G. P. Wang , L. Zhang, J. Kim, J. J. Zhang. J. *Power .Sources.* , 217 (2012) 554.
18. R. Patel, A. Inamdar, B. Hou, S. Cha, A. T. Ansari, J. Gunjakar, H. Im, H. Kim, *Curr. Appl. Phys.*, 17 (2017) 501-506.
19. T. Yan, H. Y. Zhu, R. Y. Li, Z. J. Li, J. K. Liu, G. L. Wang, Z. Q. Gu, *Electrochim. Acta.* , 111 (2013) 71.
20. T. Yan, R. Y. Li, Z. J. Li, *Mater. Res. Bull.*, 51 (2014) 97-104.
21. X. Bai, Q. Liu, H. S. Zhang, J. Y. Liu, Z. S. Li, X. Y. Jing, Y. Yuan, L. H. Liu, J. Wang, *Electrochim. Acta.*, 215 (2016) 492-499.
22. H. N. Ma, J. He, D. B. Xiong, J. S. Wu, Q. Q. Li, V. Dravid, Y. F. Zhao, *Acs. Appl. Mater. Interfaces.*, 10 (2016) 1021.
23. X. Q. Cai, X. P. Shen, L. B. Ma, Z. Y. Ji, C. Xu, A. H.Yuan, *Chem. Eng. J.*, 268 (2015) 251-259.

24. Y. Kim, E. Cho, S. J. Park, S. Kim, *J. Ind. Eng. Chem.*, 33 (2016) 108-114.
25. M. Li, J. P. Cheng, F. Liu, X. B. Zhang, *Chem. Phys. Lett.*, 640 (2015) 5-10.